

Modelling and Optimizing the Laser Parameters to Attain the Minimum Wear Rate in Nickel Based (Inconel- 625) Hardfaced Surfaces

A.Umesh Bala

Research Scholar, Department of Manufacturing Engineering, Annamalai University, Tamil Nadu, India.

Dr.R.Varahamoorthi

Associate Professor, Department of Manufacturing Engineering, Annamalai University, Tamil Nadu, India.

Abstract – In this Investigation, an attempt has been made to optimize the Laser process parameters of hardfaced surfaces such as Laser Power (P), Travel Speed (T), Defocusing Distance (D) and Powder feed rate (F) to minimize the wear rate of nickel based Inconel-625 produced on AISI 304 stainless steel. The influence of the Laser hardfacing process parameters on the Wear Rate is discussed for optimized condition. The experiments were conducted based on a four factor and five level central composite rotatable designs. The empirical relationship was developed using Response Surface Methodology (RSM) technique to predict the Wear Rate of hardfaced surfaces at 95% confidence level. The interaction effects of input process parameters of laser hardfacing surface on Wear Rate are discussed. The optimized process parameter and the influenced parameter are identified. From this investigation it is found that the minimum wear rate of 0.271578 (mg/N-km) is could be achieved by the laser power of 2507(W), travel speed of 1034(mm/min), defocusing distance of 30 (mm) and powder feed rate of 40.5(g/min).

Key words: Modeling, Optimization, RSM, Inconel-625, Laser Hardfacing, Wear rate.

1. INTRODUCTION

In the recent technologies of material surface modification, laser hardfacing is a very effective method, which can significantly improve the surface properties of material such as wear-resistance, anticorrosion, heat-resistance and antioxidant. In addition, the technology of laser hardfacing can also repair the damaged products, especially

complex metal parts. Hardfacing technology has been widely applied in industries. But there are some defects such as crack and porous which affects the quality and endurance of the product and these problem has not been solved effectively. If the selection of process parameters is improper or unmatched, the defects are easily formed on the surface and in the interior of hardfaced layer. In laser hardfacing process the Processing parameters have an essential impact on the hardfacing quality, like geometry, dilution and defects. Formerly, process tests were used to find the optimized parameters through trial and error. The Laser hardfacing process is controlled by many interlinked process parameters, which include the laser power (P), travel speed (T), defocusing distance (D) and powder feed rate (F). Inconel-625, a nickel based hardfacing powder has been widely used for various hardfacing applications in critical industries like aerospace, automobile, heat exchangers, chemical industry, electrochemical industry power generation plants, turbines, industrial boiler components of pressurized water reactors like reactor core and control rod and nuclear power plants. Out of emerging technologies laser aided direct metal deposition based on new additive manufacturing principle has been reported to achieve the hardfaced surface using Inconel as hardfacing powder are free from cracks, bonding errors and porosity. New repair technologies like laser hardfacing have been shown to be superior than the traditional TIG hardfacing and PTA hardfacing used as a main repair tool.

C	Mn	Ni	Si	P	S	Cr	Fe
≤ 0.12	≤ 2.0	8.00–11.00	≤ 1.0	≤ 0.035	≤ 0.03	17.00–19.00	Balance

Table 1: Chemical composition (wt. %) of Base material (AISI 304)

Cr	Mn	Mo	Nb	Fe	Al	Si	Ti	Mn	Ni
22.76	0.20	7.96	2.86	4.18	0.36	0.37	0.39	0.20	Balance

Table 2: Chemical composition (wt. %) of Powder material (Inconel-625)

Laser hardfacing using Inconel-625 have shown to be better performer under wear and corrosion conditions. AISI 304 stainless steel is a less expensive structural material that found applications within general wear and corrosive environments. During hardfacing process its lower carbon content reduces the precipitation of carbide in the fusion zone. Nickel-based hardfacing powder and stainless steel have extensive applications in the manufacturing of components. The hardfaced specimens were subject to the abrasive wear test on pin-on-disk wear equipment. The purpose of the wear tests was to characterize the wear properties of the laser hardfaced samples under dry conditions and to predict the wear rate of laser hardfaced surfaces.

2. EXPERIMENTAL WORK

2.1 Identify the important process variables and its limits:

The laser hardfacing, experimental runs were carried out based on trial experiments on the 14 mm-thick 304 stainless-steel plate using nickel based (Inconel-625) hardfacing powder to find out the feasible working limits of laser hardfacing parameters. The working range was decided based on the quality and the absence of any detectable defects. Different combinations of parameters were used to carry out the trial experiments. This was done by varying any one of the factors from minimum to maximum while keeping the other parameters at constant. Laser hardfaced deposit which was exposed to a smooth appearance without any visible defects such as crack, pores were chosen. The identified input laser parameters are: Laser Power (P), Travel Speed (T), Defocusing Distance (D) and Powder Feed Rate (F). The controllable process parameters for laser hardfacing equipment were identified to carry out the experimental work are noted in Table.3. The upper limit was coded as + 2 whereas the lower limit -2 by using the input parameters and their working range. The design matrix was developed and the experiments were conducted as per the design matrix.

2.2 Experimental design matrix:

The selected design matrix shown in the Table.4 was the central composite rotatable factorial design consisting 30 set of experiments. All variables at the intermediate (0) level constitute the center point while the combination of each variable at either lower value (-2) or higher value (+2) with the other variables of the intermediate level constitute the star

points. Thus the 30 experimental run of design matrix were developed to conduct the experiments.

2.3 Evaluation the wear rate of laser hardfacing surfaces:

The laser hardfacing is carried out on AISI 304 stainless steel by using CO₂ laser with a maximum capacity of 4000W as per the design matrix at random order. The average deposited thickness was about 0.8–1.6 mm of the stainless steel. After hardfacing the deposit was cut into small samples by using Electrical Discharge Machining (EDM) for wear test on pin on disc machine as shown in Figure.1. and scanned electron microcopy (SEM) images. The evaluating of wear rate for 30 samples as per the design matrix was calculated and the subsequent values are noted. The same wear rate values are used for deriving the empirical relationship.



Figure1: Laser Hardfaced Samples for wear test.

Parameters	Units	Notations	Levels				
			-2	-1	0	1	2
Laser Power	W	P	2200	2350	2500	2650	2800
Travel Speed	mm/min	T	800	900	1000	1100	1200
Defocusing Distance	mm	D	15	20	25	30	35
Powder Feed Rate	g/min	F	30	35	40	45	50

Table 3: Laser hardfacing parameters and their limits.

3. DEVELOPING AN EMPIRICAL RELATIONSHIP

Wear Rate of Laser hardfaced surface is a function of the Laser parameters such as Laser power (P), Travel speed (T), Defocusing distance (D), powder feed rate (F), and it can be expressed as

Wear Rate of Laser Hardfaced surfaces = f (P, T, D, F)

$$\begin{aligned} \text{Wear Rate} = \{ &+14.28 - 0.0069 (P) - 0.0042 (T) - 0.0334 (D) \\ &- 0.12 (F) - 2.16 \text{ E-}07 (PT) + 8.13 \text{ E-} 06 (PD) \\ &+ 6.60 \text{ E-}06 (PF) - 8.20 \text{ E-}06 (TD) + 0.000016 \\ &(TF) + 0.00036 (DF) + 1.32 \text{ E-} 06 (P^2) \\ &+ 2.14 \text{ E-}06(T^2) + 0.000086 (D^2) + 0.0010(F^2) \} \end{aligned}$$

(3)

The second-order polynomial equation used to predict the response surface Y is given by

$$Y = b_0 + \sum b_i x_i + \sum b_{ii} x_i^2 + \sum b_{ij} x_i x_j \tag{1}$$

And for four factors, the selected polynomial could be expressed equally

$$\begin{aligned} \text{Wear Rate} = \{ &b_0 + b_1(P) + b_2(T) + b_3(D) + b_4(F) + b_{12} (PT) \\ &+ b_{13} (PD) + b_{14}(PF) + b_{23}(TD) + b_{24} (TF) + b_{34} \\ &(DF) + b_{11}(P^2) + b_{22}(T^2) + b_{33}(D^2) + b_{44}(F^2) \} \end{aligned} \tag{2}$$

Where, b_0 is the mean value of the response and $b_1, b_2, b_3, \dots, b_4$ are linear, interactions and square terms of factors. The value of co-efficient was calculated using Design Expert software at 95% confidence level. The significance of the each co-efficient was calculated from t-test and p values. Which are listed in Table.5. The final empirical relationship was constructed using only these co-efficient and the established final empirical relationship of wear rate on laser hardfaced deposit of Inconel-625 alloy is given below.

The ANOVA test results are given in Table 5. at the desired confidence level of 95%. The adequacy of the above relation is tested by analysis of variance. The relationship may be considered to be adequate. The Model F-value of 77.57 implies the model is significant. There is only a 0.01% chance that an F-value, this large could occur due to noise. P-values less than 0.0500 indicate model terms are significant. In this case P, T, D, F, PD, PF, TF, DF, P^2 , T^2 , F^2 are significant model terms. Values greater than 0.1000 indicate the model terms are not significant. If there are many insignificant model terms (not counting those required to support hierarchy), model reduction may improve your model. The Lack of Fit F-value of 0.76 implies the Lack of Fit is not significant relative to the pure error. There is a 66.60% chance that a "Lack of Fit F-value" this large could occur due to noise. Non-significant lack of fit is good and we found the model to be fit. In this the Predicted R^2 of 0.9448 is in reasonable agreement with the Adjusted R^2 of 0.9737. That shows the difference is less than 0.2. Adequate Precision measures the signal to noise ratio. A ratio greater than 4 is desirable. The ratio of 30.130 indicates that the signal is an adequate signal. This model can be used to navigate the design space. The correlation graph shows in Figure:2 the predicted and actual wear rate of laser hardfaced deposit, could indicate the deviation between the actual and predicted wear rate is low.

S.No	Coded Value				Actual Value			
	Laser Power (W)	Travel Speed (mm/min)	Defocusing Distance (mm)	Powder Feed Rate (g/min)	Laser Power (W)	Travel Speed (mm/min)	Defocusing Distance (mm)	Powder Feed Rate (g/min)
1	-1	-1	-1	-1	2350.00	900.00	20.00	35.00
2	1	-1	-1	-1	2650.00	900.00	20.00	35.00
3	-1	1	-1	-1	2350.00	1100.00	20.00	35.00
4	1	1	-1	-1	2650.00	1100.00	20.00	35.00
5	-1	-1	1	-1	2350.00	900.00	30.00	35.00
6	1	-1	1	-1	2650.00	900.00	30.00	35.00
7	-1	1	1	-1	2350.00	1100.00	30.00	35.00
8	1	1	1	-1	2650.00	1100.00	30.00	35.00
9	-1	-1	-1	1	2350.00	900.00	20.00	45.00
10	1	-1	-1	1	2650.00	900.00	20.00	45.00
11	-1	1	-1	1	2350.00	1100.00	20.00	45.00
12	1	1	-1	1	2650.00	1100.00	20.00	45.00
13	-1	-1	1	1	2350.00	900.00	30.00	45.00
14	1	-1	1	1	2650.00	900.00	30.00	45.00
15	-1	1	1	1	2350.00	1100.00	30.00	45.00
16	1	1	1	1	2650.00	1100.00	30.00	45.00
17	-2	0	0	0	2200.00	1000.00	25.00	40.00
18	2	0	0	0	2800.00	1000.00	25.00	40.00
19	0	-2	0	0	2500.00	800.00	25.00	40.00
20	0	2	0	0	2500.00	1200.00	25.00	40.00
21	0	0	-2	0	2500.00	1000.00	15.00	40.00
22	0	0	2	0	2500.00	1000.00	35.00	40.00
23	0	0	0	-2	2500.00	1000.00	25.00	30.00
24	0	0	0	2	2500.00	1000.00	25.00	50.00
25	0	0	0	0	2500.00	1000.00	25.00	40.00
26	0	0	0	0	2500.00	1000.00	25.00	40.00
27	0	0	0	0	2500.00	1000.00	25.00	40.00
28	0	0	0	0	2500.00	1000.00	25.00	40.00
29	0	0	0	0	2500.00	1000.00	25.00	40.00
30	0	0	0	0	2500.00	1000.00	25.00	40.00

Table 4: Experimental Design Matrix and its actual values.

Source	Sum of Squares	Degree of Freedom	Mean Square	F-Value	p-value (Prob> F)	Significant (or) Not significant
Model	0.0649	14	0.0046	77.57	< 0.0001	Significant
P	0.0018	1	0.0018	29.64	< 0.0001	
T	0.0032	1	0.0032	54.1	< 0.0001	
D	0.0031	1	0.0031	52.41	< 0.0001	
F	0.0092	1	0.0092	153.33	< 0.0001	
PT	0.0002	1	0.0002	2.83	0.1134	
PD	0.0006	1	0.0006	9.96	0.0065	
PF	0.0004	1	0.0004	6.56	0.0217	
TD	0.0003	1	0.0003	4.5	0.051	
TF	0.001	1	0.001	16.29	0.0011	
DF	0.0014	1	0.0014	22.66	0.0003	
P ²	0.0245	1	0.0245	410.68	< 0.0001	
T ²	0.0126	1	0.0126	210.47	< 0.0001	
D ²	0.0001	1	0.0001	2.1	0.1674	
F ²	0.0173	1	0.0173	288.9	< 0.0001	
Residual	0.0009	15	0.0001			
Lack of Fit	0.0005	10	0.0001	0.7633	0.666	
Pure Error	0.0004	5	0.0001			
Cor Total	0.0658	29				
R-Squared	0.9864		Std. Dev.	0.0077		
Adj. R-Squared	0.9737		Mean	0.3472		
Pred. R-Squared	0.9448		C.V. %	2.23		
Adeq. Precision	30.1295					

Table 5: Anova Test Result

3.1 Predicted values and actual values:

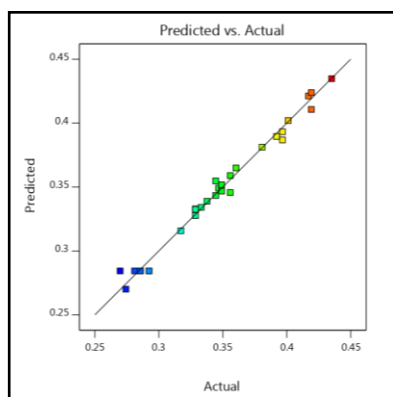


Figure 2: Correlation Graph.

4. OPTIMIZING THE LASER PARAMETERS

Response Surface Methodology or commonly known as RSM is an anthology of statistical and mathematical methods that are helpful in generating improved methods and optimizing a process. Response Surface methodology is an assortment technique useful for modeling and analyzing experiments in which a response variable is influenced by several independent variables. It explores the relationships between several independent variables and one or more response variables the response variable can be graphically viewed as a function of the process variables (or) independent variables and this graphical perspective of the problem has led to the term Response Surface Methodology. RSM is applied to fit the acquired model to the desired model when random factors are present and it may fit linear or quadratic models to describe the response in terms of the independent variables and then search for the optimal settings for the independent variables by performing an optimization step. The RSM was

constructed to check the model part accuracy which uses the built time as function of the process variables and other parameters. Central composite designs (CCD) are appropriate for calibrating the full quadratic models described in Response Surface Models. There are three types of CCD, namely, circumscribed, inscribed and faced. Each design consists of a factorial design (the corners of a cube) together with center and star points that allow estimation of second order effects. For a full quadratic model with n factors, CCD have enough design points to estimate the $(n+2) (n+1) / 2$ coefficient in a full quadratic model with n factors. The type of CCD used (the position of the factorial and star points) is determined by the number of factors and by the desired properties of the design. A design is rotatable if the prediction variance depends only on the distance of the design point from the center of the design.

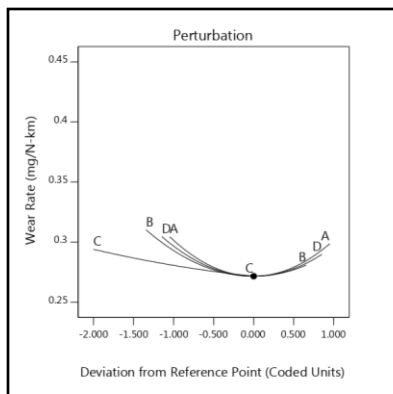


Figure 3: Perturbation Graph.

The perturbation plot in Figure.3 shows the response of Wear Rate of the laser hardfaced surface. When each Laser Hardfacing parameter transfers from the reference point, with all other parameters held constant as the orientation value. This plot offers an outline view of the response and displays the transformation of Wear Rate, The design of experiment sets the reference point by default in the middle of the design space. From the perturbation graph and response surface graphs, it can be observed that when the Wear Rate decreases with increasing Powder Feed Rate. It may be validated due to increase in hardness of laser hardfaced surface. Wear Rate increases with increasing laser power. It may be assumed that the high heat input will up turn the depth of penetration and dilution of the deposits. Contour plot shows a vital role in the erudition of the response surface. It is vibrant from that when the Wear Rate decreases with increasing Powder Feed Rate and defocusing distance. Wear Rate increases with increasing laser power, travel speed .

The surface and contour plots are shown in Figure 4 (A–F) for each process parameters. It is clear that the Wear Rate get minimized with the rise in powder feed rate (F) and defocusing distance (D). With an increase of process parameters such as laser power (P) and travel speed (T), the wear rate reaches to a minimum level and then it starts to multiples. Wear Rate mainly depends on dilution, hardness and microstructure. When the powder feed rate increases the dilution rate is minimized which because of more amount of heat is utilized for melting the hardfacing powder material and only a very small amount of heat is enough to melt the substrate material. So that the Wear Rate starts minimizing. The rate of dilution reduces with the increase of defocusing distance which leads the decrease of wear rate to certain limit. With increasing the Transfer speed, the powder density per square area becomes less hence there is an upturn in the dilution rate and it rise the value of Wear Rate. Laser power is mainly used for melting the powder but when it keeps increasing, the high volume of substrate material begins to melts which leads to the results of an upturn in dilution, as the variation of Wear Rate in laser hardfaced sample could be affected by the dilution. As the results of higher dilution the hardness of laser hardfaced sample falls down which leads to an increasement in wear rate. So the dilution should be kept minimum to attain the achievable minimum wear rate. Increasing Laser Power raises the dilution rate and multiples the Wear Rate. By analyzing the response surface and contour plots as shown in Figure 4 (A–F), the optimized rounded values of laser hardfacing parameters are shown in Table.6. It is found that the minimum wear rate of 0.271578 (mg/N-km) can be achieved by the laser power of 2507 (W), Travel speed of 1034 (mm/min), Defocusing distance of 30 (mm) and Powder feed rate of 40.5 (g/min) at the response surface plot and corresponding domain in the contour plot.

S. No	Important Laser Parameters	Optimized Value
1	Laser Power	2507 (W)
2	Travel Speed	1034 (mm/min)
3	Defocusing Distance	30 (mm)
4	Powder Feed Rate	40.5 (g/min)

Table 6: Optimized Hardfacing Parameters for wear rate.

4.1 The Response surface and contour plots:

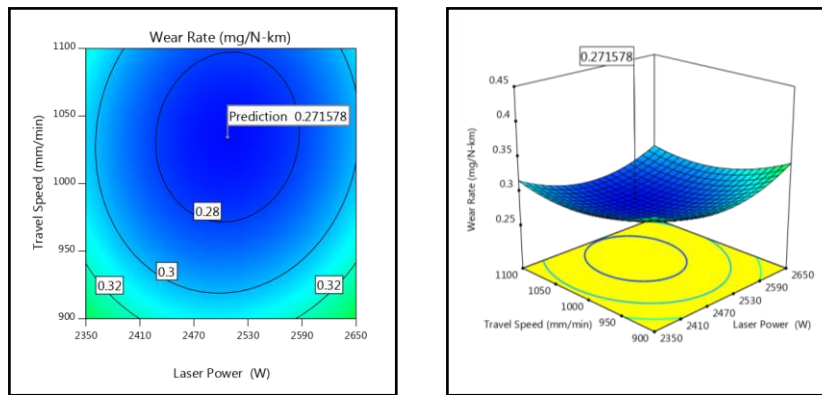


Figure 4A: Interaction effect of Laser Power and Travel Speed.

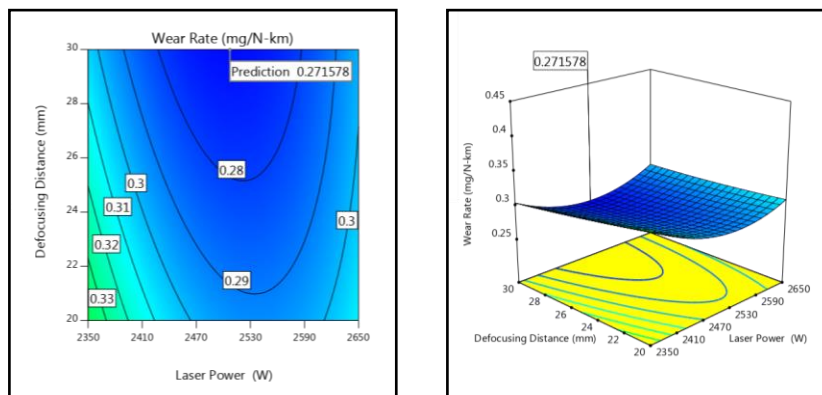


Figure 4B: Interaction effect of Laser Power and Defocusing Distance.

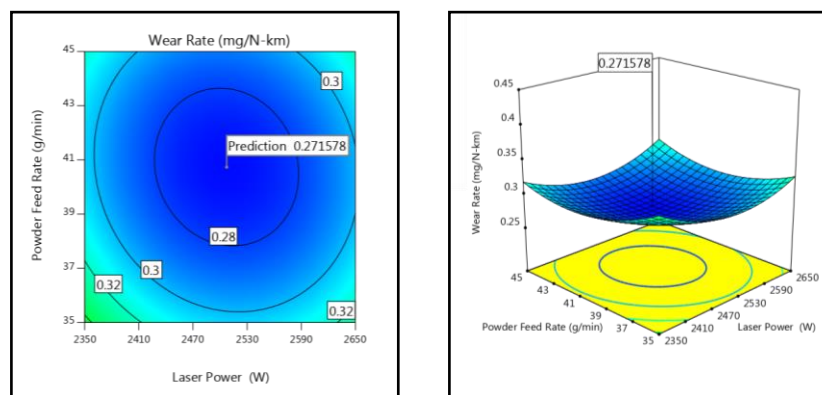


Figure 4C: Interaction effect of Laser Power and Powder Feed Rate.

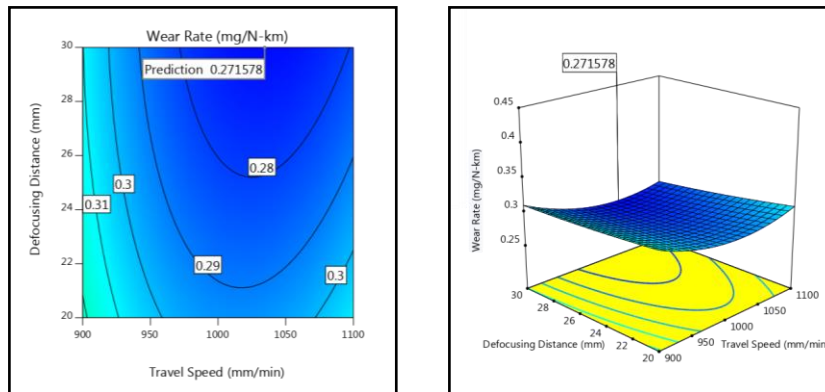


Figure 4D: Interaction effect of Travel Speed and Defocusing Distance.

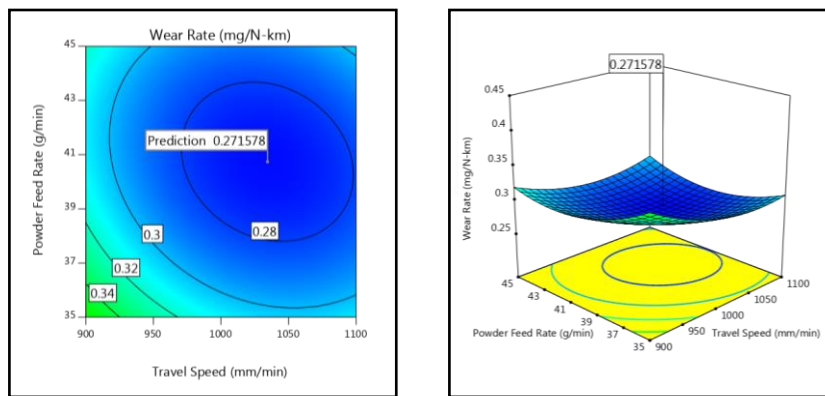


Figure 4E: Interaction effect of Travel Speed and Powder Feed Rate.

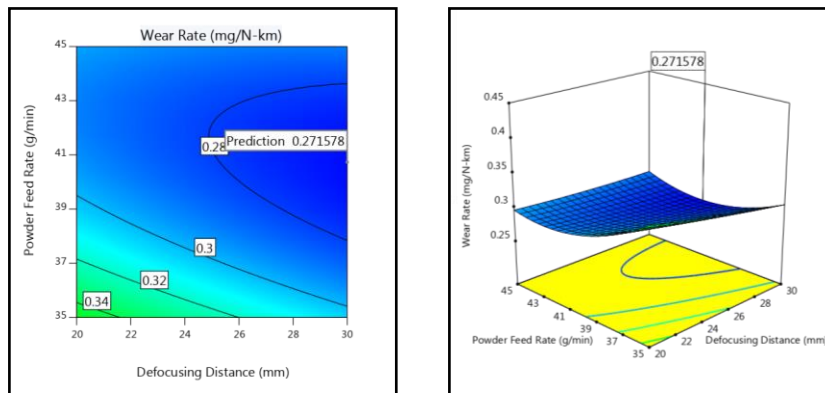


Figure 4F: Interaction effect of Powder Feed Rate and Defocusing Distance.

5. CONCLUSION

1. AISI 304 Stainless Steel plate of thickness 14 mm were hardfaced by laser successfully without defects under optimized hardfacing condition.
2. An empirical relationship was developed to predict the Wear Rate of nickel-based (Inconel-625) hardfaced layer produced on AISI 304 Stainless-Steel substrates by incorporating important Laser Hardfacing parameters such as Laser power(P), Travel speed (T), Defocusing distance (D), and Powder feed rate (F) with 95% confidence level.
3. A minimum Wear Rate of 0.271578 (mg/N-km) could be achieved in the Laser hardfaced surface which was produced by the Laser Power of 2507 (W), Travel Speed of 1034 (mm/min), defocusing distance of 30 (mm) and Powder Feed Rate of 40.5 (g/min).
4. The Powder Feed Rate is identified as the major influencing factor than other three laser hardfacing parameters to predict the Wear Rate of Hardfaced surfaces.

REFERENCES

- [1] T. E. Abioye, J. Folkes, and A. T. Clare, "A parametric study of Inconel 625 wire laser deposition," *J. Mater. Process. Technol.*, vol. 213, no. 12, pp. 2145–2151, 2013.
- [2] T. C. Chen, C. C. Chou, T. Y. Yung, K. C. Tsai, and J. Y. Huang, "Wear behavior of thermally sprayed Zn/15Al, Al and Inconel 625 coatings on carbon steel," *Surf. Coatings Technol.*, vol. 303, pp. 78–85, 2016.
- [3] G. P. Dinda, A. K. Dasgupta, and J. Mazumder, "Laser aided direct metal deposition of Inconel 625 super alloy : Microstructural evolution and thermal stability," *Mater. Sci. Eng. A*, vol. 509, no. 1–2, pp. 98–104, 2009.
- [4] F. Fu, Y. Zhang, G. Chang, and J. Dai, "Analysis on the physical mechanism of laser cladding crack and its influence factors," *Optik (Stuttg.)*, vol. 127, no. 1, pp. 200–202, 2016.
- [5] Z. Liu, J. Cabrero, S. Niang, and Z. Y. Al-Taha, "Improving corrosion and wear performance of HVOF-sprayed Inconel 625 and WC-Inconel 625 coatings by high power diode laser treatments," *Surf. Coatings Technol.*, vol. 201, no. 16–17, pp. 7149–7158, 2007.
- [6] K. Y. Luo, H. X. Yao, F. Z. Dai, and J. Z. Lu, "Surface textural features and its formation process of AISI 304 stainless steel subjected to massive LSP impacts," *Opt. Lasers Eng.*, vol. 55, pp. 136–142, 2014.
- [7] J. D. Majumdar, "Mechanical and Electro-Chemical Properties of Laser Surface Alloyed AISI 304 Stainless Steel with WC+Ni+NiCr," *Phys. Procedia*, vol. 41, no. November, pp. 335–345, 2013.
- [8] P. F. Mendez, "Welding processes for wear resistant overlays," *J. Manuf. Process.*, vol. 16, no. 1, pp. 4–25, 2014.
- [9] S. S. Sandhu and A. S. Shahi, "Metallurgical, wear and fatigue performance of Inconel 625 weld claddings," *J. Mater. Process. Technol.*, vol. 233, pp. 1–8, 2016.
- [10] S. Saqiba, R. J. Urbanica, and K. Aggarwal, "Analysis of laser cladding bead morphology for developing additive manufacturing travel paths," *Procedia CIRP*, vol. 17, pp. 824–829, 2014.
- [11] L. Sexton, S. Lavin, G. Byrne, and A. Kennedy, "Laser cladding of aerospace materials," *J. Mater. Process. Technol.*, vol. 122, no. 1, pp. 63–68, 2002.
- [12] M. Shakil, "Microstructure and hardness studies of electron beam welded Inconel 625 and stainless steel 304L," *Vacuum*, vol. 110, pp. 121–126, 2014.
- [13] D. Verdi, M. A. Garrido, C. J. Múnez, and P. Poza, "Mechanical properties of Inconel 625 laser cladded coatings: Depth sensing indentation analysis," *Mater. Sci. Eng. A*, vol. 598, pp. 15–21, 2014.
- [14] M. Vite, M. Castillo, L. H. Hernández, G. Villa, I. H. Cruz, and D. Stéphane, "Dry and wet abrasive resistance of Inconel 600 and stellite," *Wear*, vol. 258, no. 1–4 SPEC. ISS., pp. 70–76, 2005.
- [15] D. Z. Wang, Q. W. Hu, Y. L. Zheng, Y. Xie, and X. Y. Zeng, "Study on deposition rate and laser energy efficiency of Laser-Induction Hybrid Cladding," *Opt. Laser Technol.*, vol. 77, pp. 16–22, 2016.
- [16] F. Wear, O. F. Inconel, and I. N. H. Vacuum, "Fretting wear of Inconel in high vacuum," vol. 106, pp. 163–175, 1985.
- [17] F. Xu, Y. Lv, Y. Liu, F. Shu, P. He, and B. Xu, "Microstructural Evolution and Mechanical Properties of Inconel 625 Alloy during Pulsed Plasma Arc Deposition Process," *J. Mater. Sci. Technol.*, vol. 29, no. 5, pp. 480–488, 2013.